



# Magnetic Resonance Imaging of Osteochondral Lesions of the Talus: Comparison Between Small FOV Surface Coil with BLADE and Boot-Shape Coil Without BLADE

Yan Sun<sup>1</sup>, Yue Feng Hao<sup>2</sup>, Dan Hu<sup>2</sup> and Ke Fu Liu<sup>1,\*</sup>

<sup>1</sup>Department of Radiology, Affiliated Suzhou Hospital of Nanjing Medical University, Suzhou, China

<sup>2</sup>Department of Orthopaedics, Affiliated Suzhou Hospital of Nanjing Medical University, Suzhou, China

\*Corresponding author: Department of Radiology, Affiliated Suzhou Hospital of Nanjing Medical University, Suzhou, China. Email: liukefusuzhou@sina.com

Received 2018 June 09; Revised 2019 August 13; Accepted 2019 August 18.

## Abstract

**Background:** It is common for osteochondral lesions of the talus (OLT) to be associated with ankle injury, residual ankle stiffness and pain after osteochondral injuries, and OLTs are most common in the dome of the talus. Before choosing the appropriate therapy based on diagnosis, it is necessary to determine if the OLT is a stable lesion or not. More accurate diagnosis and classifications could be conducted to guide the clinical treatment.

**Objectives:** To compare the accuracy rate and diagnostic indices of proton-density fat-saturation BLADE (proprietary name for periodically rotated overlapping parallel lines with enhanced reconstruction in magnetic resonance systems from Siemens Healthcare) sequences from a small field of view (FOV) surface coil and proton-density fat-saturation sequences without BLADE in a routine FOV using a boot-shaped coil on the magnetic resonance imaging (MRI) of OLT.

**Patients and Methods:** One hundred and one patients with ankle pain for greater than 6 weeks and normal X-ray participated in this study. They were ready for diagnosis by arthroscopy and treatment following MR examination. All patients were scanned by two different methods: (a) a coronal proton-density fat-saturated sequence with BLADE using a small FOV surface coil and (b) a coronal proton-density fat-saturated sequence without BLADE using a routine FOV boot coil. In this study, the arthroscopic results were regarded as the gold standard for assessing OLTs and were used to directly compare the ability of the two different scanning methods to produce accurate findings with regard to MR imaging of OLTs.

**Results:** Of the 101 patients, 57 patients with cartilaginous injury were confirmed by the results of arthroscopy, and 44 patients were without cartilaginous injury. Forty-eight lesions had the same grade with the small FOV BLADE sequence MRI and arthroscopy, while 37 lesions had the same grade on routine FOV MRI and arthroscopy among 57 patients with cartilaginous injury. Among MR findings of 101 patients, the results of weighted Kappa, accuracy, sensitivity and specificity were 0.803, 90.10%, 84.21%, and 97.73%, respectively between small FOV and arthroscopy; 0.515, 75.25%, 64.91%, and 88.64%, respectively between routine FOV and arthroscopy. The accuracy rate, sensitivity and specificity of small FOV with BLADE were higher than routine FOV. Mc Nemar's test confirmed that the accuracy, sensitivity and specificity of small FOV BLADE were significantly better than routine FOV ( $P < 0.001$ ). Greater values of small FOV compared to routine FOV appeared in sensitivity of 0.94 vs. 0.81 (MR normal and grade I), 0.89 vs. 0.77 (MR normal and grade I - IIA), 0.90 vs. 0.74 (MR normal and grade I-IIB), 0.91 vs. 0.75 (MR normal and grade I - III) and specificity of 0.98 vs. 0.92 (MR normal and grade I), the same in specificity of 0.91 vs. 0.91 (MR normal and grade I - IIA), 0.80 vs. 0.80 (MR normal and grade I - III), only smaller in specificity of 0.60 vs. 0.80 (MR normal and grade I - IIB).

**Conclusion:** Small FOV surface coil with BLADE sequence grading of OLT demonstrated a promising accuracy rate compared with arthroscopic diagnosis.

**Keywords:** Arthroscopy, MRI, Osteochondral Lesion, Radiofrequency Coil, Talus

## 1. Background

Magnetic resonance imaging (MRI) has been used as an optimal technique for evaluating articular cartilage (1, 2). It can provide information about cartilage damage and correlates closely with arthroscopic findings (3). MRI has

greater sensitivity to cartilage and helps clarify cartilage damage (4). Thus, MRI has become a practical method for the diagnosis of osteochondral lesions of the talus (OLT) (5-7). It is common for OLT to be associated with ankle injury, residual ankle stiffness and pain after osteochondral

injuries, and OLTs are most common in the dome of the talus. Before choosing the appropriate therapy based on diagnosis, it is necessary to determine if the OLT is a stable lesion or not. Stable fragments that are not cystic in early stage lesions always merit conservative therapy. Both cartilaginous defects with fluid around the attached cartilage fragment and unattached fragments that are detected by MR usually require arthroscopy (8). In the classification of cartilage injury, radiologists depend on the integrity of the articular cartilage and the condition of the subchondral bone in several different situations. There is hope that imaging could resolve the cartilage and local edema of subchondral bone clearly enough to make the correct diagnosis and prescribe the appropriate treatment. However, diagnosis of articular cartilage lesions of the talus can be challenging. It is very hard to distinguish certain small structural characteristics of OLTs, especially with some alternative coil (knee joint coil, flexibility coil) imaging techniques.

Small field-of-view (FOV) surface coil imaging can provide a good view of articular cartilage and can help in evaluating its stability and classification. However, the use of BLADE is recommended in some joint imaging since it can improve image quality and reduce artifacts (9).

## 2. Objectives

In this study, our goal is to use the BLADE sequence with a small FOV surface coil for imaging. The objective of this study is to more accurately classify injured cartilage through improved imaging techniques.

## 3. Patients and Methods

### 3.1. Patient Enrollment

Approval for this study was obtained from the review board and ethics committee of our institution, and all enrolled patients provided written informed consent. A prospective study was conducted to probe the diagnostic accuracy of the two MR scanning methods. Inclusion criteria: (1) All patients had ankle pain for more than 6 weeks and normal X-ray and were ready for diagnosis by arthroscopy and treatment following MR examination (10); (2) All the MRI examinations were performed 180 days or less, prior to ankle arthroscopic treatment; (3) All consecutive patients who received a 1.5T MRI exam of the ankle and underwent subsequent ankle arthroscopic treatment, by a single surgeon, were included in this study. Exclusion criteria: MR imaging localization of patients was not

standard with obvious deviation or the image blur caused by motion would make it difficult to analyze the osteochondral structure. From January 2017 to February 2018, a total of 101 patients (53 males, 48 females; mean age, 45 years; range, 18 - 69 years) were enrolled in this study. All of 101 patients, the mean interval time between the MRI and arthroscopy was 2.6 (range, 0.2 to 5.7) months.

### 3.2. MRI Examination

All MR examinations were performed on a 1.5-T whole-body MRI scanner (Magnetom Avanto, Siemens Medical Solutions, Germany). The two MR scanning methods were: (a) Proton-density fat-saturation with conventional Cartesian PDFS sequences using a routine FOV boot coil ("boot coil", Suzhou Medcoil Healthcare, China, Figure 1A). The following parameters were applied: repetition time (TR)/echo time (TE) = 3500/45 ms; FOV: 220 × 220 mm; slice thickness, 3 mm; inter-slice gap, 0.3 mm. The actual spatial resolution was approximately 0.6 mm<sup>2</sup>. (b) Proton-density fat-saturation with BLADE (PDFS BLADE) sequences using a commercially available 4-cm circular polarized receiver surface coil ("finger coil", Siemens Medical Solutions, Germany, Figure 1B). The small FOV coil was taped over the lateral or medial aspect of the ankle overlying the site of the OLT. Parameters applied for small FOV imaging were as follows: TR/TE = 3500/45 ms; FOV: 100 × 100 mm; slice thickness, 2 to 3 mm; inter-slice gap, 0.2 to 0.3 mm. The actual spatial resolution was approximately 0.3 mm<sup>2</sup>. A coronal MR imaging was necessary and the sagittal plane could be used as supplementary imaging. Small FOV coil imaging with a BLADE sequence was performed after boot coil imaging in all patients.

### 3.3. Study Design and Articular Cartilage Analysis

All MRI exams were evaluated side-by-side by the two radiologists (reader 1 with 14 years and reader 2 with 11 years of experience in musculoskeletal radiology) and a consensus reached in all cases (when they encountered controversial cases, the two radiologists reached a consensus through consultation) that eliminated any potential inter-observer variability. Both radiologists were blinded to the results of the arthroscopic findings. These OLTs were evaluated and classified based on MRI by applying the Berndt and Harty classification: I, subchondral compression fracture with intact overlying articular cartilage; IIA, subchondral cyst; IIB, partially detached osteochondral fragment; III, the osteochondral fragment is completely detached but is not displaced; IV, the osteochondral fragment is detached and displaced. One of these two radi-

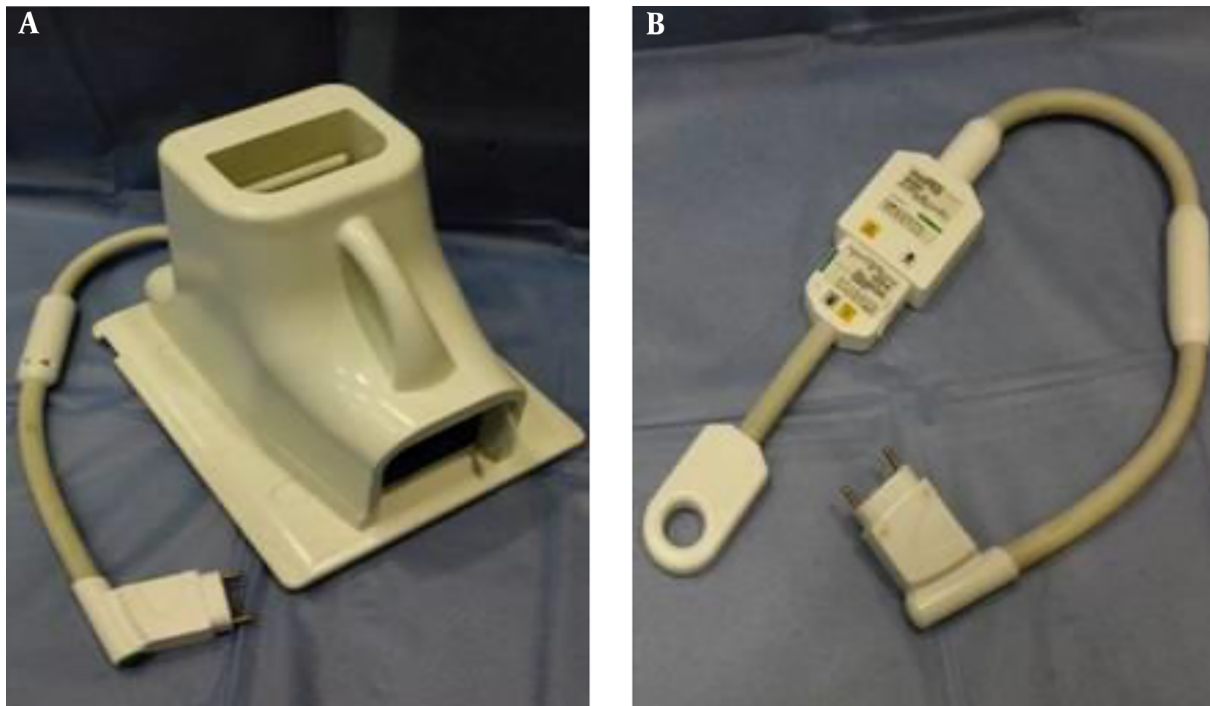


**Figure 1.** A, A boot-shaped coil. It is commercially available from Suzhou Medcoil Healthcare China. B, A 4-cm small field of view (FOV) surface coil. It is commercially available from Siemens Medical Solutions, Germany.

ologists (reader 1) repeated this grading assessment two weeks later to determine intra-observer variation.

All arthroscopic examinations were performed by a single orthopedic surgeon. The arthroscopic results were graded using the following criteria: A, smooth and intact but soft and ballotable cartilage; B, rough surfaces; C, fibrillations or fissures; D, flap present or bone exposed; E, loose, undisplaced fragment; F, displaced fragment (11).

Arthroscopic results were regarded as the gold standard for assessing OLTs in this study. Classification results from two MR methods were compared with the conclusions of arthroscopic examinations. The corresponding relationship between MR and arthroscopic results was described with the following criteria: (1) arthroscopic grade A = MR grade I; (2) arthroscopic grade B and C = MR grade IIA; (3) arthroscopic grade D = MR grade IIB; (4) arthroscopic grade E = MR grade III (5) arthroscopic grade F = MR grade IV.

The entire process is as shown in the flowchart (Figure 2).

#### 3.4. Statistical Analysis

All data were analyzed using IBM SPSS Statistics for Windows, version 24.0 Released 2016 (SPSS Inc., Chicago, Ill.,

USA). A level of  $P < 0.05$  was considered statistically significant. Weighted kappa coefficient was computed to compare the degree of agreement of each MRI method with gold standard. Values from 0.0 to 0.19 indicate slight agreement, 0.20 to 0.39 indicate fair agreement, 0.40 to 0.59 indicate moderate agreement, 0.60 to 0.79 indicate substantial agreement, and 0.80 to 1.0 indicate almost perfect or perfect agreement. For the overall samples and classified samples, McNemar's was performed to test the differences between the two methods in the diagnostic accuracy rate, sensitivity and specificity.

The arthroscopic grading represents the increasing severity of OLTs from normal, grade A to grade F, so we handled this matter by dichotomization of the grades in both arthroscopy and MRI in five different situations. The first step towards performing the case study was to combine grade B and C arthroscopy. These dichotomizations for arthroscopy will be normal vs. grades A - F, normal and grade A vs. grades B - F, normal and grades A - C vs. grades D - F, normal and grades A - D vs. grades E - F and normal and grades A - E vs. grade F. Their corresponding MRI dichotomizations will be normal vs. grades I - IV, normal and grade I vs. grades IIA - IV, normal and grades I - IIA vs. grades

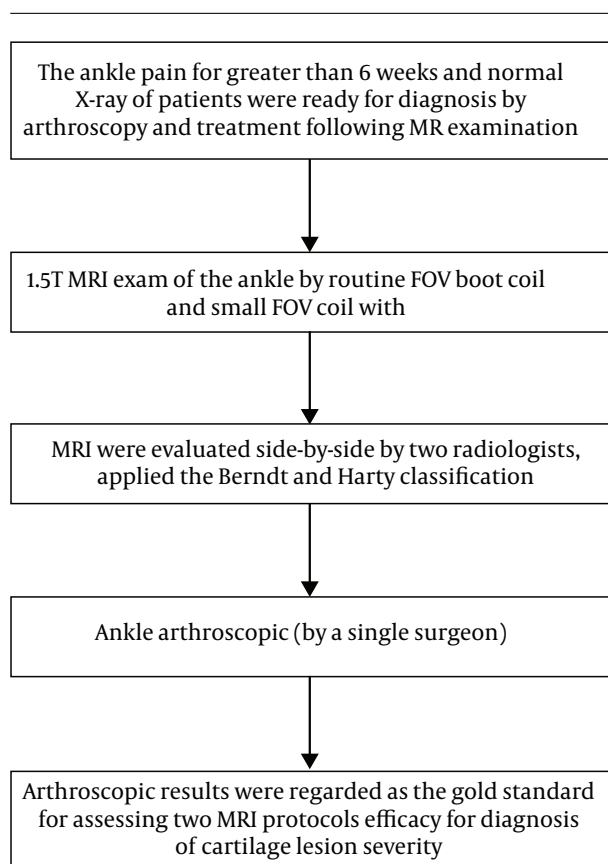


Figure 2. Flowchart of patients' enrollment

IIB - IV, normal and grades I - IIB vs. grades III - IV and normal and grades I - III vs. grade IV. In each dichotomization, we constructed the  $2 \times 2$  cross tables and calculated all diagnostic indices with 95% confidence intervals.

#### 4. Results

The results of arthroscopy (101 patients): 57 patients with cartilaginous injury and 44 patients without cartilaginous injury, there were eight cases of arthroscopic grade A, 14 of grade B = 8 and C = 6, 20 of grade D, 10 of grade E, and 5 of grade F. For small FOV surface coil PDFS BLADE, among the 57 patients with OLTs, 48 patients had the same grade for both MRI and arthroscopy, 43 patients were correctly diagnosed without OLTs (total 44 patients without OLTs). For routine FOV boot coil PDFS, among the 57 cases, 37 lesions had the same grade for both MRI and arthroscopy, 39 patients were correctly diagnosed without OLTs (total 44 patients without OLTs). The results of weighted Kappa were 0.803 (95% confidence interval [CI] = 0 - 0.35) between

small FOV and arthroscopy, 0.515 (95% CI = 0 - 0.36) between routine FOV and arthroscopy.

First, the overall sample was estimated. The diagnosis accuracy of small FOV BLADE (90.10%, 91/101, 95% CI = 0.842 - 0.960) was higher than routine FOV (75.25%, 76/101, 95% CI = 0.667 - 0.838). Mc Nemar's test revealed a statistically significant difference ( $P < 0.001$ , 95% CI = 3.93 - 14.69) in the diagnosis accuracy between two methods. Sensitivity and specificity of small FOV with BLADE were higher than routine FOV. According to arthroscopic findings, sensitivity and specificity of small FOV BLADE was 84.21% (95% CI = 0.72 - 0.92), and 97.73% (95% CI = 0.86 - 0.99) and routine FOV was 64.91% (95% CI = 0.51 - 0.77), and 88.64% (95% CI = 0.75 - 0.96), respectively. The results of the Mc Nemar's test showed significant differences in the sensitivity ( $P < 0.001$ , 95% CI = 1.98 - 8.52) and specificity ( $P < 0.001$ , 95% CI = 5.36 - 283.87) between the two methods.

Second, arthroscopic results were gold standard in this study. The corresponding relationship between MR and ankle arthroscopy showed the summarized results. The results of the 49 positive cases from small FOV method: there were six cases of MR grade I, 10 of grade IIA, 18 of grade IIB, 10 of grade III, four of grade IV and one false positive. The 42 positive cases from routine FOV method: there were three cases of MR grade I, nine of grade IIA, 13 of grade IIB, eight of grade III, four of grade IV and five false positive. These calculated diagnostic indices of small FOV BLADE and routine FOV with gold standard were chosen based on the diagnostic indices regarding sensitivity (Sen), specificity (Spec), positive predictive value (PPV), negative predictive value (NPV), positive likelihood ratio (PLR), negative likelihood ratio (NLR), and accuracy. For 57 patients with cartilaginous injury, the results for classifications of arthroscopy and MRI in five different dichotomizations have been described in Table 1.

#### 5. Discussion

The thickness of articular cartilage on the dome of talus has been demonstrated to be only 0.4 to 2.1 mm (12). In the absence of sufficient joint fluid, the cartilage closely approximates the distal tibial articular cartilage (13), making it very difficult to make a precise evaluation using MRI (11, 14). Subchondral trabecular compression on the talar dome is difficult to detect when the compression amplitude is slight. Marrow edema and subchondral cysts show an equal or high signal intensity beneath lesions on proton density (PD)-weighted images. This makes MRI evaluation more challenging, especially in distinguishing be-

**Table 1.** Diagnostic Indices of Small FOV and Routine FOV<sup>a</sup>

	i (SF)	i (RF)	ii (SF)	ii (RF)	iii (SF)	iii (RF)	iv (SF)	iv (RF)	v (SF)	v (RF)
<b>Sen (95% CI)</b>	0.98 (0.86 - 0.99)	0.89 (0.75 - 0.96)	0.94 (0.83 - 0.98)	0.81 (0.67 - 0.90)	0.89 (0.79 - 0.95)	0.77 (0.65 - 0.86)	0.90 (0.81 - 0.95)	0.74 (0.64 - 0.83)	0.91 (0.83 - 0.95)	0.75 (0.65 - 0.83)
<b>Spec (95% CI)</b>	0.84 (0.72 - 0.92)	0.65 (0.51 - 0.77)	0.98 (0.88 - 0.99)	0.92 (0.80 - 0.97)	0.91 (0.76 - 0.98)	0.91 (0.76 - 0.98)	0.60 (0.33 - 0.83)	0.80 (0.51 - 0.95)	0.80 (0.30 - 0.99)	0.80 (0.30 - 0.99)
<b>PPV (95% CI)</b>	0.83 (0.69 - 0.91)	0.66 (0.53 - 0.78)	0.98 (0.88 - 0.99)	0.91 (0.78 - 0.97)	0.95 (0.86 - 0.99)	0.94 (0.84 - 0.99)	0.93 (0.84 - 0.97)	0.96 (0.87 - 0.99)	0.99 (0.93 - 0.99)	0.99 (0.92 - 0.99)
<b>NPV (95% CI)</b>	0.98 (0.88 - 0.99)	0.88 (0.74 - 0.96)	0.94 (0.83 - 0.98)	0.82 (0.69 - 0.90)	0.82 (0.66 - 0.92)	0.68 (0.53 - 0.80)	0.50 (0.27 - 0.73)	0.35 (0.20 - 0.54)	0.31 (0.10 - 0.61)	0.14 (0.05 - 0.34)
<b>PLR (95% CI)</b>	6.19 (3.39 - 11.29)	2.53 (1.75 - 3.65)	46.2 (6.63 - 321.64)	9.89 (3.83 - 25.54)	10.43 (3.52 - 30.87)	9.02 (3.03 - 26.81)	2.24 (1.20 - 4.18)	3.72 (1.34 - 10.32)	4.53 (0.78 - 26.19)	3.75 (0.65 - 21.73)
<b>NLR (95% CI)</b>	0.03 (0.004 - 0.19)	0.18 (0.08 - 0.41)	0.06 (0.02 - 0.18)	0.21 (0.12 - 0.37)	0.12 (0.06 - 0.23)	0.25 (0.16 - 0.39)	0.17 (0.09 - 0.35)	0.32 (0.22 - 0.47)	0.12 (0.06 - 0.24)	0.31 (0.20 - 0.49)
<b>Accuracy (95% CI)</b>	0.90 (0.84 - 0.96)	0.75 (0.67 - 0.84)	0.96 (0.92 - 0.99)	0.86 (0.79 - 0.93)	0.90 (0.84 - 0.96)	0.82 (0.75 - 0.90)	0.85 (0.78 - 0.92)	0.75 (0.67 - 0.84)	0.90 (0.84 - 0.96)	0.75 (0.67 - 0.84)

Abbreviations: CI, confidence interval; FOV, field of view; NLR, negative likelihood ratio; NPV, negative predictive value; PLR, positive likelihood ratio; PPV, positive predictive value; RF, routine FOV; SF, small FOV

<sup>a</sup>These dichotomizations for MRI corresponding arthroscopy: i, (normal vs. grades A-F) and (normal vs. grades I-IV); ii, (normal-grade A vs. grades B-F) and (normal-grade I vs. grades II-IV); iii, (normal-grades A-C vs. grades D-F) and (normal-grades I-IIA vs. grades IIB-IV); iv, (normal-grades A-D vs. grades E-F) and (normal-grades I-IIB vs. grades III-IV); v, (normal-grades A-E vs. grade F) and (normal-grades I-III vs. grade IV).

tween MR grade I and grade IIA (Figure 3). Small FOV imaging helps optimize resolution of the talar dome articular cartilage, providing a better signal-to-noise ratio even at 1.5T MRI than standard MRI at 3T (15, 16).

This study may be the first to date to apply the BLADE sequence with a small FOV coil in ankles with talar dome osteochondral lesions. The results of this study indicate that the small FOV surface coil BLADE sequence showed the cartilage better than a routine FOV boot coil sequence (Figure 4). There are several reasons for the differences between the two techniques, and the first is due to the effects of different coils. A small FOV coil was closely fixed to the location of cartilage injury with tape. This allows for more effective imaging due to reduced distance and signal loss. The design of the boot coil was in accordance with the anatomical structure of the ankle. However, considering individual differences, there must be a certain distance between the joint surface and the coil, resulting in reduced signal strength. The second reason is the difference in FOV. The difference in spatial resolution is easily visible. The actual spatial resolution was higher (0.3 mm<sup>2</sup>) in small FOV sequences than in routine FOV sequences (0.6 mm<sup>2</sup>). In addition to the approximately two-fold improvement in spatial resolution, Antonio et al. (16) reported that use of a small FOV coil significantly enhanced the MR signal to approximately double within the focus region compared to that for extremity coil imaging. The third factor is the application of the BLADE technique. The conventional k-space trajectory is a Cartesian pattern; the collected data is filled into the k-space line-by-line. BLADE is

the product name of the Siemens Medical System (Erlangen, Germany) turbo-spin echo (TSE) sequence that uses the periodically-rotated overlapping parallel lines with enhanced reconstruction (PROPELLER) k-space trajectory. The BLADE method acquires many blades that are rotated around the center of the k-space. Each blade is composed of many of the lowest-phase encoding lines of a conventional rectangular k-space trajectory that are acquired after a single radio frequency excitation (17). The central region of k-space is repeatedly filled with the rotating rectangular data matrix. In theory, the main role of the central region of k-space is to determine the image contrast, so we have reason to believe that image contrast is clearly improved because of the multiple data fillings in the central region of k-space. Based on our results, it was found that BLADE sequences improved image contrast in all cases, although the general role of the BLADE sequence was to eliminate motion artifacts. Compared with the conventional sequence, the visualization of joint fluid with the BLADE sequence showed higher signal intensity. Therefore, we had better contrast between joint fluid and cartilage, so implementation of the BLADE sequence improved diagnostic accuracy in our study (Figure 5).

Comparing the results with similar studies, our test results indicated that there were obvious improvements in all the accuracies, sensitivities and most of the specificities by using the small FOV BLADE sequence. In a study conducted by Lee et al., they could increase the joint space width with traction in small FOV coil. Although this method can improve the cartilage surface visibility



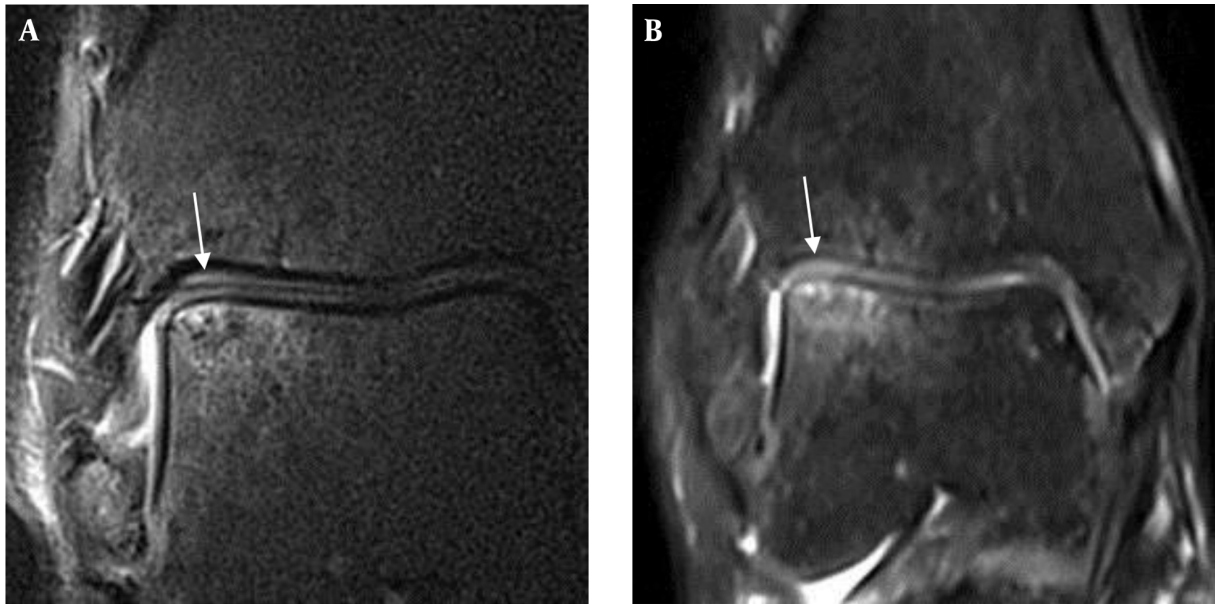


**Figure 3.** A, The extent of edema and the morphology of cartilage in the talar dome can be visualized on the small FOV PDFS BLADE image (MR grade I). B, Routine FOV PDFS image shows the osteochondral lesion of the talus (OLT) with several small areas of cystic edema in less detail, and the cartilage of talar dome is blurry. It is classified as MR grade IIA.



**Figure 4.** A, On the small FOV PDFS BLADE image, the partial cartilage rupture of the talar dome is seen with the marrow edema and slight pitting of the subchondral bone (MR grade IIB). B, Routine FOV PDFS image shows equal or high signal edema, but the cartilage surface is unclear (MR grade I).

of talar dome, the risk is still potential (15). The results of some published studies show that MRI has the ability to display osteochondral lesions of the talus with accuracies ranging from 65.9% to 83.0% (18-20). In this study, we

came to the following conclusions: the total rate of correct classification was relatively high (90.1%) in the small FOV BLADE sequence group and relatively low (75.25%) in the routine FOV sequence group. Study results show that

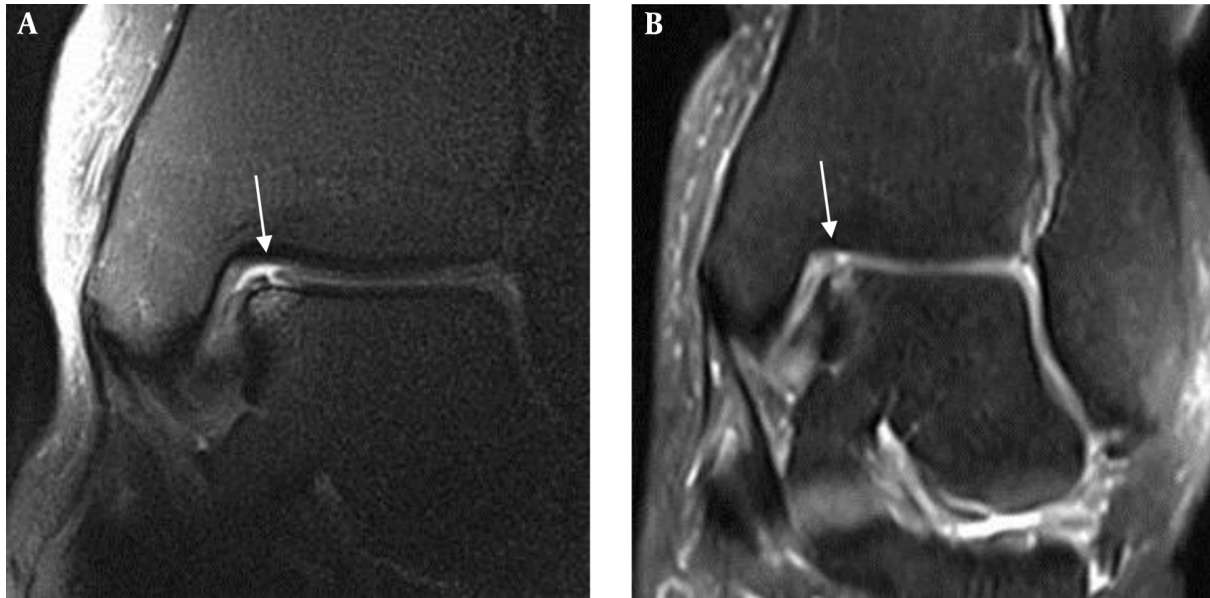


**Figure 5.** The small FOV PDFS BLADE image clearly shows a partially isolated cartilage of talar dome (MR grade IIB) (A), which is not clearly shown (MR grade IIA) on the routine FOV PDFS image (B). Improved contrast between cartilage and joint fluid with the bright signal makes it easy to assess the osteochondral lesion of the talus (OLT) situation on the small FOV BLADE image.

the small FOV has good performance on the sensitivity and specificity. The small FOV for an overall sensitivity and specificity were higher than the findings (sensitivity 84.21%, specificity 97.73%) by Gatlin et al. The difference could be due to the fact that the lesions were only grades III and IV in their report (21). Bauer and colleagues also investigated the use of MRI in the detection of cartilage lesions of the ankle. Their results show that sensitivity (71%) and specificity (> 95%) were different from our study. The major reasons for the differences may be because the lesions were artificially manufactured in a cadaver model (22).

The main limitation of the current study is that first, the difference in accuracy is caused by spatial resolution, different coils and BLADE sequence together. However, we did not analyze the influence degree of each single factor to the final outcome, we just discovered the differences between two methods of imaging. Second, the corresponding relationship between MR classification (the Berndt and Harty) and the arthroscopic results are not absolutely matched, only a relatively reasonable choice that has been used in a professional paper (18). Third, patients with mild cartilage injuries rarely undergo arthroscopy. For MR grade I osteochondral lesions, the small FOV BLADE sequence was great for improving the accuracy rate, but only a small number of patients were included in our study, and no significant differences could be detected be-

tween the two methods.

In conclusion, small FOV BLADE sequence grading of osteochondral lesions in the talus was useful and had a promising accuracy rate with respect to arthroscopic classification.

#### Footnotes

**Authors' Contributions:** Study conception and design: Yan Sun, Ke Fu Liu and Yue Feng Hao; acquisition of data: Yan Sun, Dan Hu; analysis and interpretation of data: Yan Sun and Ke Fu Liu; drafting of manuscript: Yan Sun; critical revision: Yan Sun and Ke Fu Liu

**Conflict of Interests:** None declared.

**Ethical Approval:** Ethics Committee approval was obtained from the Institutional Ethics Committee of Affiliated Suzhou Hospital of Nanjing Medical University to the commencement of the study, and all enrolled patients provided written informed consent (ethical approval code: KL901011).

**Financial Disclosure:** There is not any financial disclosure.

**Funding/Support:** This study was supported by the project of Jiangsu provincial commission of health and family planning (Z201612), Jiangsu youth medical talents

(QNRC2016236), Jiangsu high level health professional project (LGY2017010), Jiangsu Natural Science Foundation (BK20181179).

## References

- Disler DG, McCauley TR, Kelman CG, Fuchs MD, Ratner LM, Wirth CR, et al. Fat-suppressed three-dimensional spoiled gradient-echo MR imaging of hyaline cartilage defects in the knee: Comparison with standard MR imaging and arthroscopy. *AJR Am J Roentgenol*. 1996;**167**(1):127-32. doi: [10.2214/ajr.167.1.8659356](https://doi.org/10.2214/ajr.167.1.8659356). [PubMed: [8659356](https://pubmed.ncbi.nlm.nih.gov/8659356/)].
- Disler DG, Recht MP, McCauley TR. MR imaging of articular cartilage. *Skeletal Radiol*. 2000;**29**(7):367-77. doi: [10.1007/s002560000222](https://doi.org/10.1007/s002560000222). [PubMed: [10963421](https://pubmed.ncbi.nlm.nih.gov/10963421/)].
- Ferkel RD, Flannigan BD, Elkins BS. Magnetic resonance imaging of the foot and ankle: correlation of normal anatomy with pathologic conditions. *Foot Ankle*. 1991;**11**(5):289-305. doi: [10.1177/107110079101100506](https://doi.org/10.1177/107110079101100506). [PubMed: [1674712](https://pubmed.ncbi.nlm.nih.gov/1674712/)].
- Lusse S, Claassen H, Gehrke T, Hassenpflug J, Schunke M, Heller M, et al. Evaluation of water content by spatially resolved transverse relaxation times of human articular cartilage. *Magn Reson Imaging*. 2000;**18**(4):423-30. doi: [10.1016/s0730-725x\(99\)00144-7](https://doi.org/10.1016/s0730-725x(99)00144-7). [PubMed: [10788720](https://pubmed.ncbi.nlm.nih.gov/10788720/)].
- Linklater JM. Imaging of talar dome chondral and osteochondral lesions. *Top Magn Reson Imaging*. 2010;**21**(1):3-13. doi: [10.1097/RMR.0b013e31820efc2](https://doi.org/10.1097/RMR.0b013e31820efc2). [PubMed: [21317564](https://pubmed.ncbi.nlm.nih.gov/21317564/)].
- O'Connor MA, Palaniappan M, Khan N, Bruce CE. Osteochondritis dissecans of the knee in children. A comparison of MRI and arthroscopic findings. *J Bone Joint Surg Br*. 2002;**84**(2):258-62. doi: [10.1302/0301-620x.84b2.11823](https://doi.org/10.1302/0301-620x.84b2.11823). [PubMed: [11922369](https://pubmed.ncbi.nlm.nih.gov/11922369/)].
- Tan TC, Wilcox DM, Frank L, Shih C, Trudell DJ, Sartoris DJ, et al. MR imaging of articular cartilage in the ankle: Comparison of available imaging sequences and methods of measurement in cadavers. *Skeletal Radiol*. 1996;**25**(8):749-55. doi: [10.1007/s002560050173](https://doi.org/10.1007/s002560050173). [PubMed: [8958622](https://pubmed.ncbi.nlm.nih.gov/8958622/)].
- De Smet AA, Fisher DR, Burnstein MI, Graf BK, Lange RH. Value of MR imaging in staging osteochondral lesions of the talus (osteochondritis dissecans): Results in 14 patients. *AJR Am J Roentgenol*. 1990;**154**(3):555-8. doi: [10.2214/ajr.154.3.2106221](https://doi.org/10.2214/ajr.154.3.2106221). [PubMed: [2106221](https://pubmed.ncbi.nlm.nih.gov/2106221/)].
- Lavdas E, Mavroidis P, Hatzigeorgiou V, Roka V, Arikidis N, Oikonomou G, et al. Elimination of motion and pulsation artifacts using BLADE sequences in knee MR imaging. *Magn Reson Imaging*. 2012;**30**(8):1099-110. doi: [10.1016/j.mri.2012.04.001](https://doi.org/10.1016/j.mri.2012.04.001). [PubMed: [22673894](https://pubmed.ncbi.nlm.nih.gov/22673894/)].
- DeSmet AA, Dalinka MK, Alazraki N, Berquist TH, Daffner RH, el-Khoury GY, et al. Chronic ankle pain. American College of Radiology. ACR Appropriateness Criteria. *Radiology*. 2000;**215** Suppl:321-32. [PubMed: [11037444](https://pubmed.ncbi.nlm.nih.gov/11037444/)].
- Ferkel RD, Zanotti RM, Komenda GA, Sgaglione NA, Cheng MS, Applegate GR, et al. Arthroscopic treatment of chronic osteochondral lesions of the talus: Long-term results. *Am J Sports Med*. 2008;**36**(9):1750-62. doi: [10.1177/0363546508316773](https://doi.org/10.1177/0363546508316773). [PubMed: [18753679](https://pubmed.ncbi.nlm.nih.gov/18753679/)].
- Dipaola JD, Nelson DW, Colville MR. Characterizing osteochondral lesions by magnetic resonance imaging. *Arthroscopy*. 1991;**7**(1):101-4. doi: [10.1016/0749-8063\(91\)90087-e](https://doi.org/10.1016/0749-8063(91)90087-e). [PubMed: [2009106](https://pubmed.ncbi.nlm.nih.gov/2009106/)].
- Griffith JF, Wang YX, Lodge SJ, Wong MW, Ahuja AT. Small field-of-view surface coil mr imaging of talar osteochondral lesions. *Foot Ankle Int*. 2010;**31**(6):517-22. doi: [10.3113/FAI.2010.0517](https://doi.org/10.3113/FAI.2010.0517). [PubMed: [20557818](https://pubmed.ncbi.nlm.nih.gov/20557818/)].
- Mintz DN, Tashjian GS, Connell DA, Deland JT, O'Malley M, Potter HG. Osteochondral lesions of the talus: A new magnetic resonance grading system with arthroscopic correlation. *Arthroscopy*. 2003;**19**(4):353-9. doi: [10.1053/jars.2003.50041](https://doi.org/10.1053/jars.2003.50041). [PubMed: [12671617](https://pubmed.ncbi.nlm.nih.gov/12671617/)].
- Lee RKL, Griffith JF, Law EKC, Ng AWH, Yeung DKW. Ankle traction during MRI of talar dome osteochondral lesions. *AJR Am J Roentgenol*. 2017;**209**(4):874-82. doi: [10.2214/AJR.17.17873](https://doi.org/10.2214/AJR.17.17873). [PubMed: [28705062](https://pubmed.ncbi.nlm.nih.gov/28705062/)].
- Antonio GE, Griffith JF, Yeung DK. Small-field-of-view MRI of the knee and ankle. *AJR Am J Roentgenol*. 2004;**183**(1):24-8. doi: [10.2214/ajr.183.1.1830024](https://doi.org/10.2214/ajr.183.1.1830024). [PubMed: [15208102](https://pubmed.ncbi.nlm.nih.gov/15208102/)].
- Lavdas E, Vlychou M, Zaloni E, Vassiou K, Tsagkalis A, Dailiana Z, et al. Elimination of motion and pulsation artifacts using BLADE sequences in shoulder MR imaging. *Skeletal Radiol*. 2015;**44**(11):1619-26. doi: [10.1007/s00256-015-2232-3](https://doi.org/10.1007/s00256-015-2232-3). [PubMed: [26306388](https://pubmed.ncbi.nlm.nih.gov/26306388/)].
- Bae S, Lee HK, Lee K, Lim S, Rim NJ, Kim JS, et al. Comparison of arthroscopic and magnetic resonance imaging findings in osteochondral lesions of the talus. *Foot Ankle Int*. 2012;**33**(12):1058-62. doi: [10.3113/FAI.2012.1058](https://doi.org/10.3113/FAI.2012.1058). [PubMed: [23199853](https://pubmed.ncbi.nlm.nih.gov/23199853/)].
- Cuttica DJ, Smith WB, Hyer CF, Philbin TM, Berlet GC. Osteochondral lesions of the talus: Predictors of clinical outcome. *Foot Ankle Int*. 2011;**32**(11):1045-51. doi: [10.3113/FAI.2011.1045](https://doi.org/10.3113/FAI.2011.1045). [PubMed: [22338953](https://pubmed.ncbi.nlm.nih.gov/22338953/)].
- Dheer S, Khan M, Zoga AC, Morrison WB. Limitations of radiographs in evaluating non-displaced osteochondral lesions of the talus. *Skeletal Radiol*. 2012;**41**(4):415-21. doi: [10.1007/s00256-011-1242-z](https://doi.org/10.1007/s00256-011-1242-z). [PubMed: [21826614](https://pubmed.ncbi.nlm.nih.gov/21826614/)].
- Gatlin CC, Matheny LM, Ho CP, Johnson NS, Clanton TO. Diagnostic accuracy of 3.0 Tesla magnetic resonance imaging for the detection of articular cartilage lesions of the talus. *Foot Ankle Int*. 2015;**36**(3):288-92. doi: [10.1177/1071100714553469](https://doi.org/10.1177/1071100714553469). [PubMed: [25253576](https://pubmed.ncbi.nlm.nih.gov/25253576/)].
- Bauer JS, Barr C, Henning TD, Malfair D, Ma CB, Steinbach L, et al. Magnetic resonance imaging of the ankle at 3.0 Tesla and 1.5 Tesla in human cadaver specimens with artificially created lesions of cartilage and ligaments. *Invest Radiol*. 2008;**43**(9):604-11. doi: [10.1097/RLI.0b013e31817e9ada](https://doi.org/10.1097/RLI.0b013e31817e9ada). [PubMed: [18708853](https://pubmed.ncbi.nlm.nih.gov/18708853/)].